RJC

RASĀYAN *J. Chem.*
Vol. 11 | No. 4 |1405 - 1414| October - December | 2018
ISSN: 0974-1496 | e-ISSN: 0976-0083 | CODEN: RJCABP
http://www.rasayanjournal.com
http://www.rasayanjournal.co.in

SYNTHESIS OF WO_3 NANORODS AND THEIR PHOTOCATALYTIC DEGRADATION OF ORGANIC CONTAMINANTS

T. Jeyapaul[1], K. Prakash[2], S. Harikengaram[3], A. Chellamani[4] and V. Selvam[1,*]

[1]Department of Chemistry, The MDT Hindu College, Affiliated to Manonmaniam Sundaranar University Tirunelveli-627010, Tamil Nadu, India
[2]Department of Chemistry, VHNSN College, Virudhunagar-626001, Tamil Nadu, India
[3]Department of Chemistry, PMT College, Tirunelveli, Tamil Nadu, India
[4]Department of Chemistry, Manonmaniam Sundaranar University, Tirunelveli, Tamil Nadu, India
*E-mail: selvam.che@gmail.com

ABSTRACT

In this present investigation, we report a novel tungsten trioxide (WO_3) nanorods were successfully synthesized by the simple hydrothermal environment. The as-synthesized rod-like WO_3 were characterized by various spectroscopic and analytical techniques such as X-ray diffraction (XRD) UV-vis spectroscopy analysis (UV-DRS). The structural morphology and their elements were confirmed by scanning electron microscopy (SEM) and energy-dispersive X-ray spectroscopy (EDX). It was found that the rod-like structure of WO_3 was successfully confirmed by transmission electron microscopy (TEM). The synthesized WO_3 exhibits an excellent photocatalytic activity which may be attributed to the improved charge separation and complete degradation of RhB dye solution within 70 min. The photocatalyst efficiency was further tested towards the effect of dye concentration and effect of different catalyst weight. The involvement of .OH in the photocatalytic reaction was evidenced using radical quenching experiment with employing different scavengers. A possible degradation mechanism was proposed for the semiconductors and possible reasons for the enhancement of visible-light photocatalytic efficiency were discussed. This study could provide a new approach to construct a novel photocatalysts and a promising candidate catalyst for poisonous wastewater treatment in the near future.

Keywords: WO_3, hydrothermal, RhB dye, photocatalyst, the mechanism

INTRODUCTION

Driven by increasing environmental pollution and the growing threat of the current energy crisis, the search for cost-effective, sustainable and green energy sources to meet global energy demands has attracted considerable research attention[1]. Utilization of solar energy to complete degradation of organic pollutants using highly effective photocatalyst has long been considered the ultimate solution because semiconductor-based photocatalysis is an ambient temperature and green chemical process[2]. In the past few decades, metal oxides[3-5] metal sulfides[6] and bismuth-based[7] and Ag-based compounds were extensively developed for photocatalytic applications[8]. Among semiconductors, metal oxides were one type of attractive and promising material owing to their abundance, low cost, nontoxic, and relatively high chemical stability[9].Among them, WO_3 also showed excellent optical, gas-sensing properties and chemical stability, which was wide, used in sensors, solar cells and lithium-ion batteries.[10-15] However, it was difficult to respond to visible light because of its wide band gap, so the studies on the photocatalytic behavior of WO_3 under visible light irradiation had rarely been reported. Therefore, development of visible light active WO_3 is an important concern to the researchers.

Rasayan J. Chem., 11(4), 1405-1414(2018)
http://dx.doi.org/10.31788/RJC.2018.1143076

CrossMark

Recent years, many efforts have been devoted to synthesize 1D WO_3 nanostructures *via* various routes such as the sol-gel process, spray pyrolysis, pulsed laser ablation, chemical vapor deposition and thermal evaporation.[16-18] Nevertheless, many of those synthetic methods have some limitations such as need high vacuum and reaction temperature or complicated reaction processing steps. High temperatures are usually responsible for undesired particle growth and may decrease the surface areas and increase particle sizes.
Herein we report a novel simple hydrothermal route for the synthesis of a visible light active WO_3 photocatalyst for the photodegradation of RhB dye solution for the first time from the best of our authors. The prepared WO_3 were characterized by XRD, TEM, SEM, and UV and discussed in detail. The prepared WO_3 photocatalyst exhibited improved photocatalytic performance towards the degradation of RhB. The photocatalyst efficiency was further tested towards the dye concentration, catalyst dosage, and different scavengers of the dye solution.

EXPERIMENTAL

Chemicals

Sodium tungstate, Sodium Chloride, Hydrochloric acid, Rhodamine B were purchased from Sigma-Aldrich and used as such without any further purification.

Synthesis of WO_3 Nanorods

The WO_3 nanorod was prepared by the simple hydrothermal environment. In a typical synthesis, 1.527 g of $NaWO_4.2H_2O$ and 0.351 g of NaCl were dissolved into 20 mL of deionized water and then 3 mL of 2 M HCl solution was added and vigorous stirring for 30 minutes. Subsequently, the resulting light sky blue solution was transferred into a Teflon-lined sealed stainless steel autoclave at 180 °C for 48 h. Then, the precipitate was washed with copious amount of DI water and absolute ethanol and then dried at 60 °C for 12 h.

Photocatalytic Activity of WO_3 Nanorods

X-Ray Diffraction measurements were carried out using a Bruker D8 diffractometer with Cu-Ka radiation (l = 1.540598 Å) in the angular range of 10–80° (2θ) with an accelerating voltage of 40 kV and a current of 20 mA. The morphology, particle size and chemical composition of the product were examined by scanning electron microscopy (SEM VEGA3 TESCAN) and transmission electron microscopy(TEM, JEM-2100, and JEOL, JAPAN). PL spectra were measured using room temperature photoluminescence with a 325 nm He-Cd laser excitation wavelength (Shimadzu RF-5301). Shimadzu diffuse reflectance UV–Vis-1800 spectrometer was used to analyze the nanomaterials (Scheme-1).

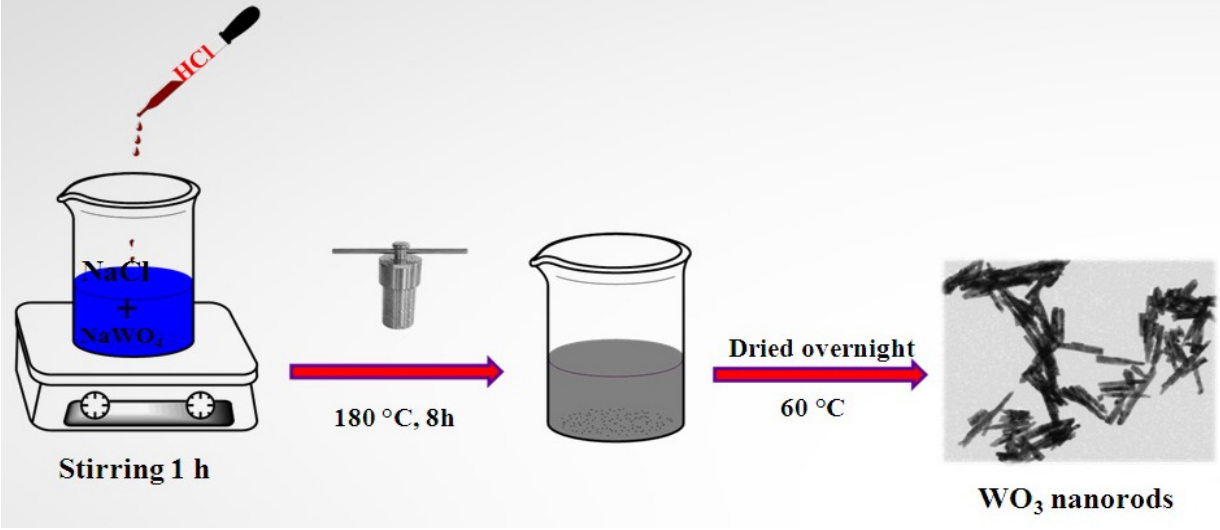

Scheme-1: Schematic Diagram of Synthesized of WO_3 Nanorods

Evaluation of Photocatalytic Activity

The photocatalytic activity of WO_3 nanorods was evaluated towards the degradation of RhB dye solution under visible light irradiation (>450 nm). A Heber photoreactor was used to the photodegradation reaction. (A 300 W tungsten incandescent lamp was used as visible light source). 50 mg of WO_3 photocatalyst was added to 75 mL of the RhB dye solution in 150 mL reaction vessel. At given time intervals, 5 mL of aliquots were collected. The degraded solutions were analyzed using the absorption peaks at 664 nm. Prior to irradiation, the suspensions were magnetically stirred in the dark condition for 1 h to ensure the equilibrium of the working solution.

RESULTS AND DISCUSSION

Structural Analysis

The phase and crystalline nature of the as-synthesized WO_3 nanorods were investigated by XRD and are shown in Fig.-1. The WO_3 Monoclinic phase was well matched with the standard JCPDS Card No 83-0950 [19]. The characteristic 2θ regions of 16.86, 24.34, 25.96, 33.58, 34.13, 35.38, 39.21, 42.95, 46.01and 49.89 were corresponds to (110), (200), (012), (202), (220), (122), (112), (032), (312) and (400) planes indicating the crystalline nature of WO_3. Especially, the XRD pattern preferred (012) orientation which has the higher intensity suggested that the WO_3 nanorods grown along the (012) plane. Any other phases are not detected in the above results indicated the high purity of the as-synthesized WO_3 nanorods.

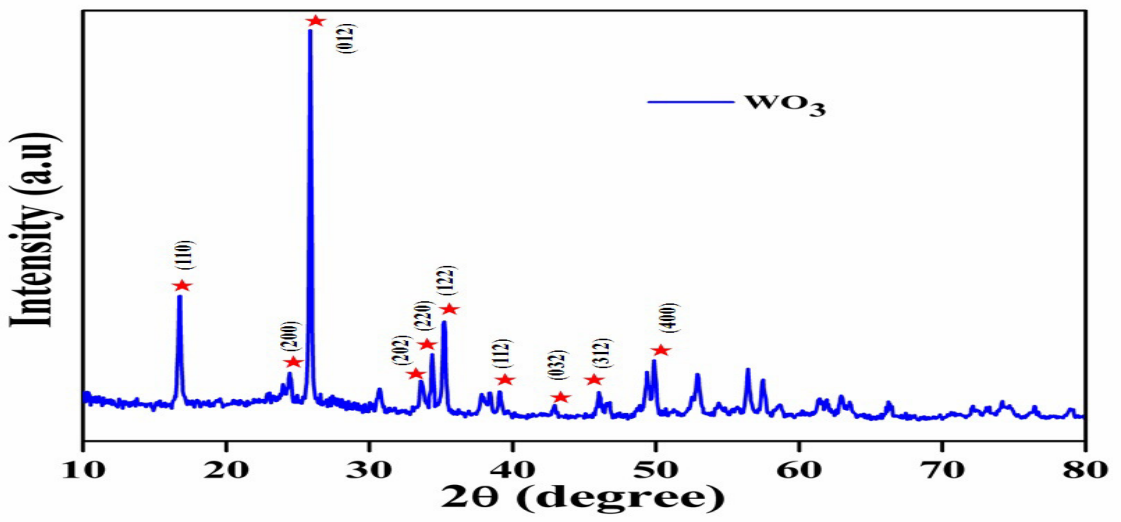

Fig.-1: XRD Patterns of Synthesized WO_3 Nanorods

The average crystallite size D, was calculated using the well known Debye Scherrer's equation[20], as:

$$D = \frac{k\lambda}{\beta Cos\theta} \qquad (1)$$

Where, D is the crystalline size, λ is the wavelength of the X-ray, β is the (Full Width at Half Maximum) FWHM of the diffraction peak, θ is the diffraction angle and k is the Scherrer's constant of the order of unity. The average crystalline sizes of the synthesized WO_3 nanorods were around 36.26 nm.

Morphological Analysis

The morphology and microstructure of the as-synthesized WO_3 were investigated by SEM and TEM as shown in Fig.-2. The SEM micrographs of synthesized WO_3 were seemed to be rod-like structures with the particle size about 200 nm which is shown in Fig.-2a. Interestingly, (Fig.-2b) the SEM micrographs synthesized WO_3 clearly showed that a numerous rod-like structures. Fig 2(c-d) shows TEM images of WO_3 nanorods with the diameter range about 20-30 nm with the calculated value is approximately 35 nm. This result is in good agreement with the XRD pattern.

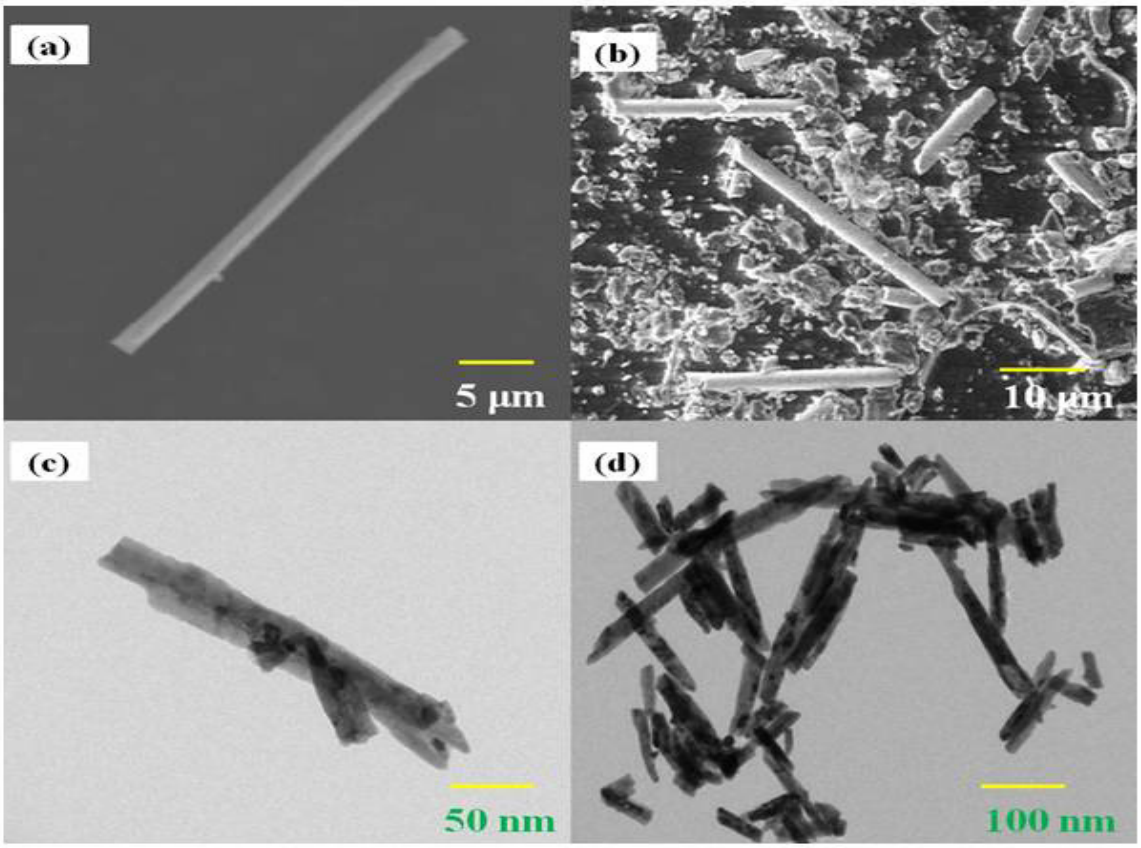

Fig.-2: (a-b) SEM Micrographs of Synthesized WO_3, (c-d) TEM Images of Synthesized WO_3 Nanorods

EDAX and Elemental Mapping Analysis

The composition of elements present in the as-synthesized WO_3 nanorods was analyzed by energy dispersive X-ray (EDX) analysis which is shown in Fig.-3. The EDX results clearly indicated that the WO_3 nanorod contains only W and O with the weight percentage of 26.52% and 73.48%, respectively. No other elements were present in the WO_3 nanorods which suggested the purity of the synthesized photocatalyst. In addition, Fig.-4 shows the composition of the elements present in the WO_3 nanorods were solid evidenced by elemental mapping analysis. These results well confirmed the presence of tungsten and oxygen is uniformly distributed in the WO_3 nanorods.

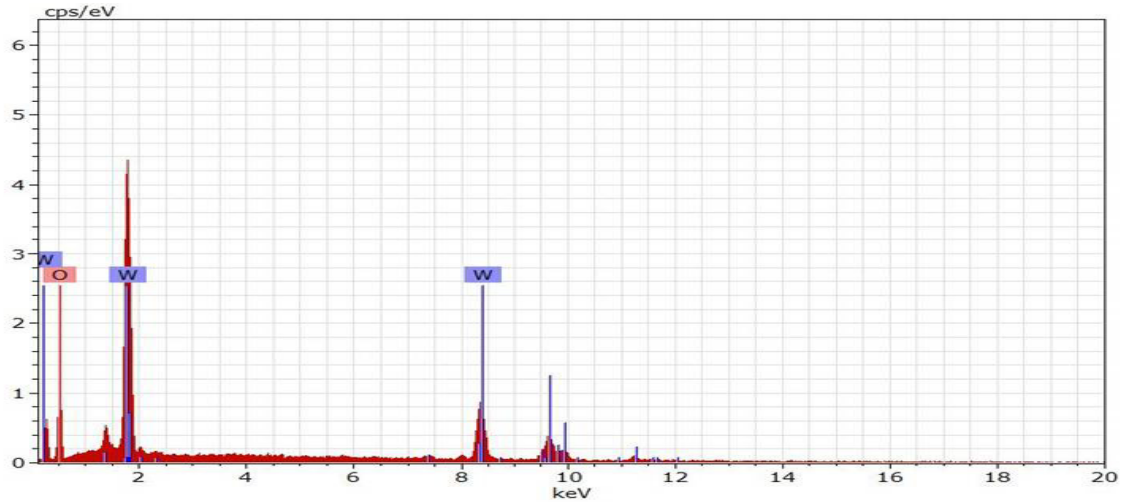

Fig.-3: EDX Spectrum of the Synthesized WO_3 Nanorods

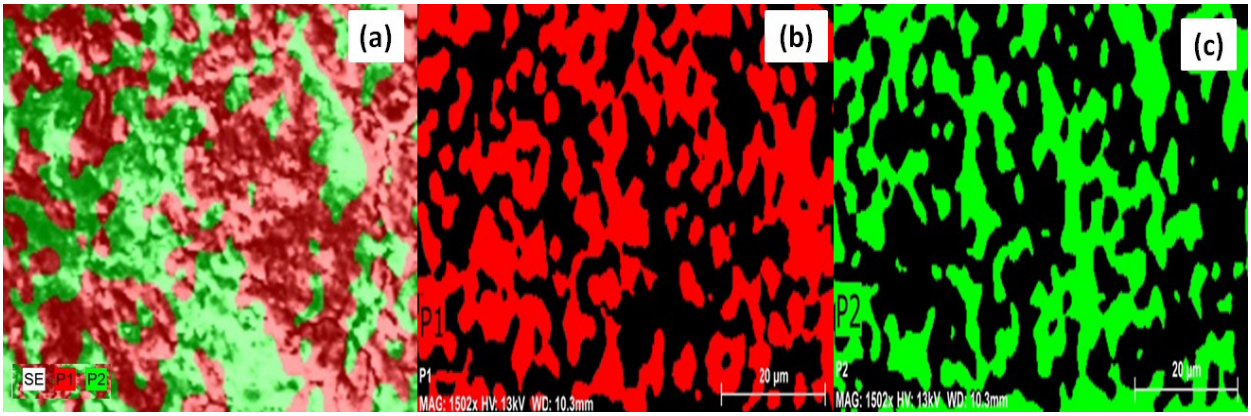

Fig.-4: (a) Elemental Mapping Images of Synthesized WO_3, (b) Tungsten, (c) Oxygen

Optical Properties

The optical absorption properties of the synthesized WO_3 are a vital parameter for the selection of the right kind of light needed for the degradation of the organic dye solution. It displayed that, WO_3 nanorods Sharpe absorption steep edges at about 375 nm in the range of visible light Fig.-5a. The band gap energy value was calculated by using Tauc's plots relationship which relates the absorption coefficient and incident photon energy of WO_3. The equation is given below:

$$(\alpha h\upsilon)^2 = A(h\upsilon - E_g)^n \quad (2)$$

Therefore, the band gap for WO_3 nanorods, a plot of $(\alpha h\upsilon)^2$ is plotted against the photon energy ($h\upsilon$) was calculated and displayed in Fig.-5b. The direct band gap energy was estimated by extrapolating the line segment of the plot $(\alpha h\upsilon)^2$ vs $h\upsilon$ to zero absorption co-efficient value. The calculated band gap energy of the WO_3 nanorods was extrapolated lines and the values about 2.7 eV and hence the WO_3 nanorods can be used as an excellent photocatalyst for the degradation of dyes under visible light irradiation[21].

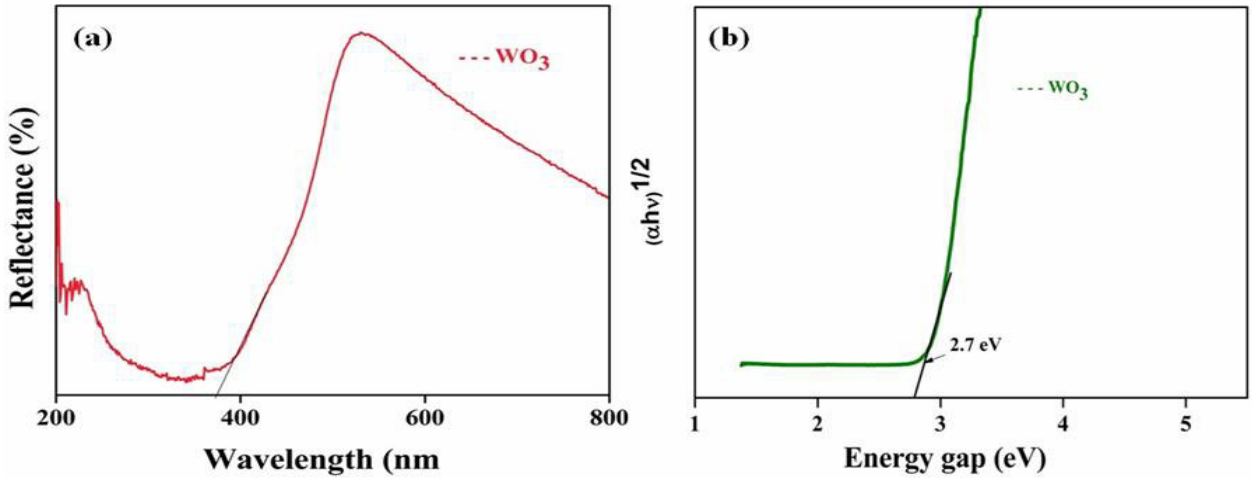

Fig.-5: (a) UV-Vis Spectra (DRS Mode) of WO_3 Nanorods and (b) Tauc's Plot of WO_3 Nanorods

The PL spectrum correlated with movement of electron transfer efficiency, in order that it can reflect photogenerated electron-hole pair separation capacity of the charge carriers. The strong PL intensity indicates the faster recombination rate of the photoexcited electron-hole combine and a lower PL intensity expresses a depressed recombination rate and hence a longer lifetime of the charge carriers. The excitation wavelength for PL spectra of WO_3 was set at 375 nm which is shown in Fig.-6. The main emission peak is centered at about 450 nm for pristine WO_3 indicating that the electron-

hole pair separation rapidly[22,23]. The WO_3 nanorods showed improved charge transport characteristic which may facilitate charge transfer.

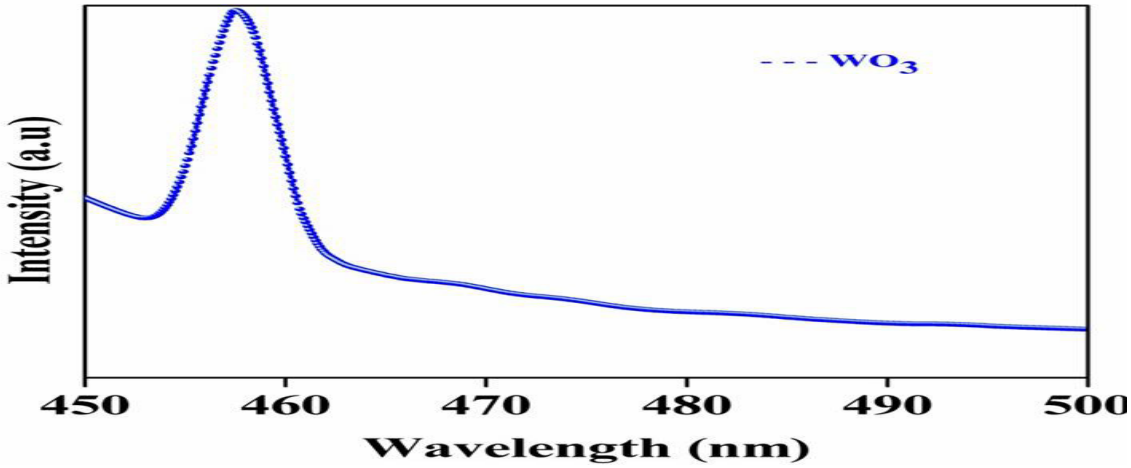

Fig.-6: Photoluminescence Spectrum of Synthesized WO_3 Nanorods

Photocatalytic Activity

The photocatalytic activity of the synthesized WO_3 nanorods was evaluated on photocatalytic degradation of Rhodamine B (RhB) dye solution under visible light irradiation shown in Fig.-7. The photo degradation of the dye was monitored by the absorption peak at 556 nm which are shown in Fig.-7. The dye was completely degraded within 70 min and the degradation percentage has been reached almost 95%. These results prompted that WO_3 nanorods can act as an excellent photocatalyst for the degradation of the dye solution.

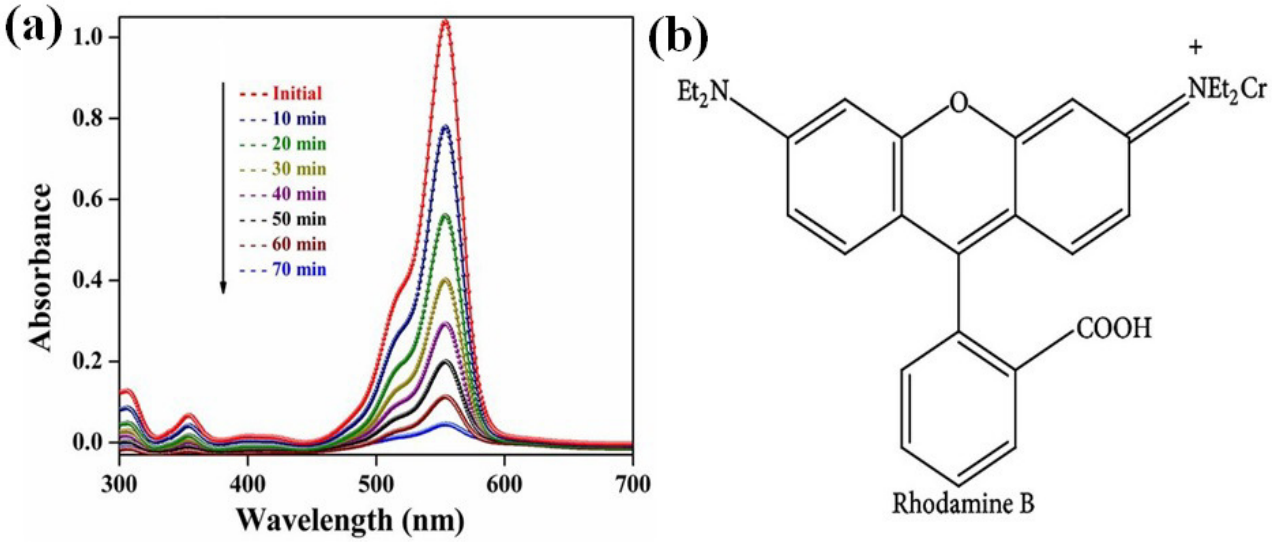

Fig.-7: Absorption Spectra of a Solution of RhB in the Presence of WO_3 Photocatalyst (50mg) under Exposure to Visible Light (b) Structure of RhB Dye

Effect of Dyes Concentration

The effect of concentration of RhB dye on the photocatalytic degradation was studied by different the dye concentration from 5 *ppm* to 20 *ppm* was shown in Fig.-8. The photocatalytic rate was high when the concentration of dye is low and vice *versa* while increasing the concentration of dye, more molecules of dye are accessible for the excitation and degradation. When the concentration of dye increases from 10 to 20 *ppm*, the rate of photodegradation decreased due to the reduced interaction of photons with the active site and thereby reduces the light intensity reached on the photocatalyst surface.[24]

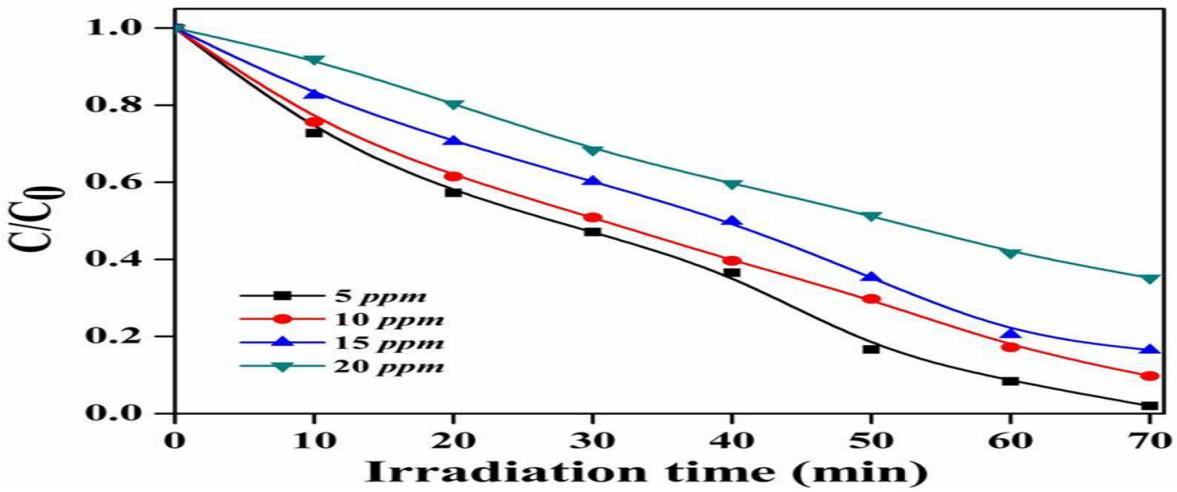

Fig.-8: Photodegradation of RhB with Different Dye Concentration in the Presence of WO_3 Photocatalyst

Effect of Catalyst

To investigate the effect of the catalyst loading on the degradation of RhB the amount of WO_3 varied from 10 to 75 mg. The photodegradation rate of the dye solution at a different amount of WO_3 shown in Fig.-9. The photodegradation rate was high when the amount of WO_3 was 50 mg. The catalyst with 5 mg of loading produces the highest photodegradation rate of dye. Amount of WO_3 below 50 mg, produces fewer holes with unit time and can produce lesser high active sites on the catalyst surface, and hence the photodegradation rate is lower. Whereas the amount of WO_3 above 50 mg, the solution becomes very turbid which prevent light passage and in turn increase the light scattering. Thus, the 50 mg of the photocatalyst is the optimum amount of photocatalytic degradation.[25]

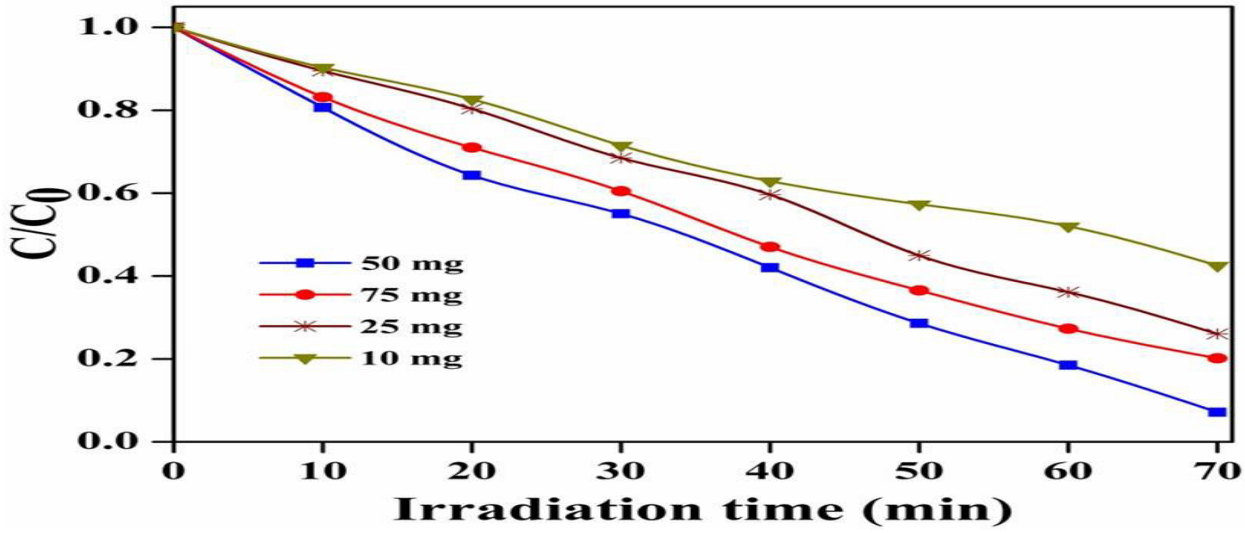

Fig.-9: Photodegradation of RhB with Different Catalyst Amount in the Presence of WO_3 Photocatalyst

Detection of Reactive Oxygen Species

Photodegradation of dyes by the semiconductor is usually completed by photoexcited electrons and holes together. On the basis of that, a series of reactive species like hydroxyl radical, active holes and superoxide radicals generated. The effect of different scavengers on the photocatalytic degradation of dye solutions was investigated to find out the reactive oxidative species involved in the mechanism. The hydroxyl radical (•OH) scavenger, benzoic acid (BA) were used to detect the involvement of •OH in the photocatalytic reaction. It was found that the degradation rate of RhB

was suppressed upon the addition of BA which suggested the involvement of OH. Triphenylphosphene (TPP), azide ion (AZ) and acrylamide (AA) are the singlet oxygen generator and superoxide radical anion (O_2•–) quencher respectively, which enhanced the rate of photocatalytic reaction proceeds by the O_2 •– [26,27]. In the present study, the rate of photodegradation was affected by a catalytic scavenger. BA shows the involvement of •OH and TPP, AZ and AA shows the involvement of O_2 •–in the degradation of RhB which is shown in Fig.-10. These results show that the photocatalytic degradation was preceded by the involvement of •OH as well as O_2•–.

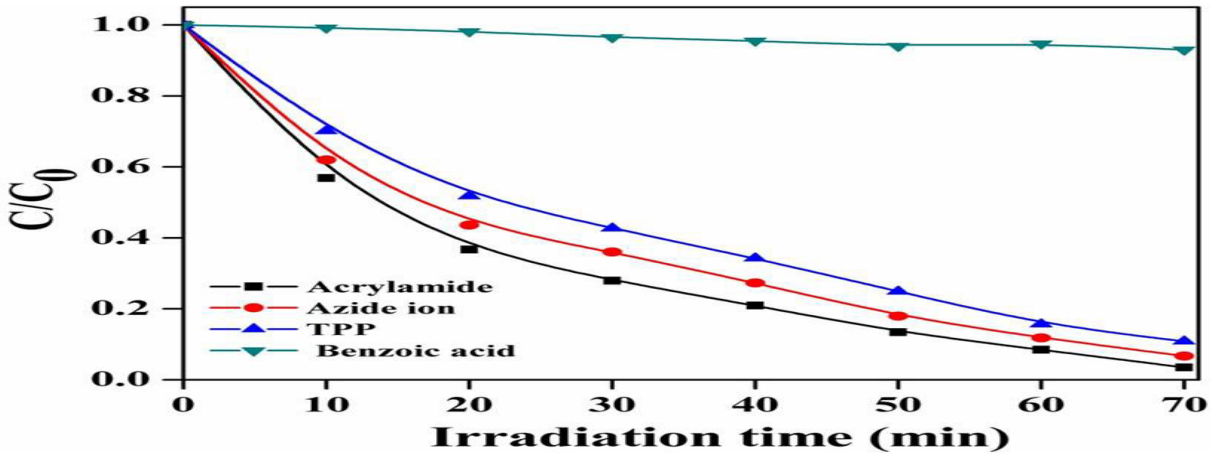

Fig.-10: Photodegradation of RhB with Different Scavengers in the Presence of WO_3 Photocatalyst

Photocatalytic Degradation Mechanism

On the basis of the experimental results and from the literature, the photocatalytic degradation mechanism of RhB dye solution by the WO_3 photocatalyst under visible light irradiation was proposed by Equations (3) to (8), as follows:

$$WO_3 + hv \rightarrow WO_3(h^+_{(vb)} + e^-_{(cb)}) \quad (3)$$

$$WO_3(e^-_{(cb)}) + O_2 \rightarrow WO_3 + O_2^- \quad (4)$$

$$O_2^- + H^+ \rightarrow .HO_2 \quad (5)$$

$$WO_3(e^-_{(cb)}) + .HO_2 + H^+ \rightarrow H_2O_2 \quad (6)$$

$$H_2O_2 + WO_3(e^-_{(cb)}) \rightarrow .OH + OH^- \quad (7)$$

$$O_2^-/OH + \text{dye} \rightarrow \text{mineralized products} \quad (8)$$

Upon irradiation of WO_3 photocatalyst under visible light an electron (e_{cb}-) in the VB was excited to the CB, and a hole (h_{vb}+) was generated in the VB simultaneously (Equation (3)). The electrons at the photocatalyst surface were inhibited by the ubiquitously present molecular oxygen to yield first the superoxide radical anion,.O_2 (Equation (4)). The superoxide radical anion .O_2 further combined with H to generate .HO (Equation (5)). The .OH radical can be formed from the trapped electron after formation of the .HO_2 radical (Equations (7) and (8)). Lastly, the photocatalytic degradation of the dyes can take place through Equation (8). The active oxygen species (.OH, .HO_2 or.O_2 radicals) or the h_{vb}+ attacked the dyes, and the dyes were degraded gradually. For example, the basic dye adsorbs the proton and protonates and this protonation continues and the degraded products are obtained after the certain period of time.

Stability of the Photocatalyst

The stability of the synthesized photocatalyst was evaluated by the recycling test and the results are shown in Fig.-11 . The photocatalyst showed radically stable even after its fifth cycle run. The

results showed that the photocatalytic activity of the WO_3 nanorods was decreased in the third cycle and subsequently maintained relative stability. The decreased percentage in degradation might be due to the adsorption of intermediate products on the active photocatalyst sites which rendered them unavailable for the photodegradation of the fresh dye solution.

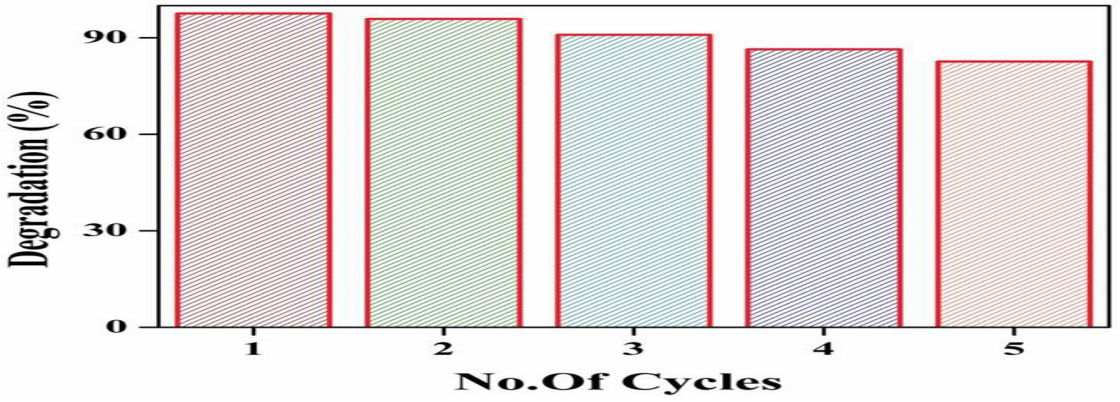

Fig.-11: Reusability of WO_3 Photocatalyst as A Function of Percentage

CONCLUSION

Novel WO_3 nanorods were prepared by simple and efficient hydrothermal method. The synthesized WO_3 nanorods were analyzed in detail. The WO_3 nanorods exhibited superior crystallinity and excellent photocatalytic activity. In addition, hydroxyl radical and superoxide radical ion were proved to be main reactive species in the photodegradation of dye RhB solution. Photocatalytic activity is very sensitive when particles are small, which is important in photocatalytic degradation and lowering the number of charge carrier recombination. The photocatalyst also displayed good stability during photodegradation and its capability to be used in several experimental cycles. The present results show that WO_3 nanorods are a promising material with high reactivity and stability for the photodegradation of dye solution under visible light irradiation.

REFERENCES

1. Z.L .Wang and W.Z. Wu, *Angew. Chem.*, **51** 11700 (2012).
2. H. Tong, S.X. Ouyang, Y.P. Bi, N. Umezawa, M. Oshikiri, and J.H. Ye, *Adv. Mater.,* **24** 229 (2011), **DOI:** 10.1002/adma.201102752
3. M.R. Hoffmann, S.T. Martin, W. Choi, and D.W. Bahnemann, *Chem. Rev.,* **95(1)**, 69(1995), **DOI:**10.1021/cr00033a004
4. A.W. Xu, W.Y. Gao, and H.Q. Liu, *J. Catal.,* **207**, 151(2002), **DOI:**10.1006/jcat.2002.3539
5. R. Nagarjuna, S. Challagulla, P. Sahu, S. Roy, R. Ganesan, *Adv. Powder. Technol.*, **28**, 3265 (2017), **DOI:**10.1016/j.apt.2017.09.030
6. M. Kudo and Y. Miseki, *Chem. Soc. Rev.*, **38,** 253(2009), **DOI:**10.1039/B800489G
7. S. Tokunaga, H. Kato, and A. Kudo, *Chem. Mater.*, **13**, 4624 (2001), **DOI:**10.1021/cm0103390
8. S. Zhang, J. Li, X. Wang, Y. Huang, M. Zeng, J. Xu, *ACS Appl. Mater. Interfaces*, **6,** 22116 (2014), **DOI:**10.1021/am505528c
9. S. Adhikari, D. Sarkar, H.S. Maiti, *Mater. Res. Bull.*, **49**, 325(2014), **DOI:**10.1016/j.materresbull.2013.08.028
10. R. Karthik, J.V. Kumar, S. M. Chen, T. Kokulnathan, H. Yang, V. Muthuraj, *ACS. Sustain. Chem. Eng.*, 6,8615, 2018, **DOI:** 10.1021/acssuschemeng.8b0093
11. J.V. Kumar, R. Karthik, S. M. Chen, N. Karikalan, K. Chelladurai, C. C. Yang, V. Muthuraj, *Nano. Micro. Lettl.*, **10**, 15652 (2018), **DOI:** 10.1021/acsami.8b00625.
12. J. V. Kumar, R.Karthik, S. M. Chen, V. Muthuraj, K. Chelladurai, *Sci. Rep.*, **6**, 34149 (2016), **DOI:**10.1038/srep34149.

13. J. V. Kumar, R. Karthik, S. M. Chen, K. H. Chen, S. Sakthinathan, V. Muthuraj, T. W. Chiu, *Chem. Eng. J.*, **346**, 11(2018), **DOI:**10.1016/j.cej.2018.03.183
14. R. Karthik, J. V. Kumar, S. M. Chen, K. Chelladurai, V. Muthuraj, *ACS Appl. Mater. Interfaces*, **9**, 6547(2017), **DOI:** 10.1021/acsami.6b14242.
15. T. Peng, D. Ke, J. Xiao, L. Wang, J. Hu, L. Zan, *J. Solid State Chem.,* **194,** 250(2012), **DOI:**10.1016/j.jssc.2012.05.016.7
16. Z. Jiao, J. Wang, L. Ke, X. W. Sun, H. V. Demir, *ACS Appl. Mater. Interfaces*, **3,** 229(2011), **DOI:** 10.1021/am100875z
17. Y. Zhang, Y. Chen, H. Liu, Y. Zhou, R. Li, M. Cai, X. Sun, *J. Phy. Chem. C,* **113** 1746(2009), **DOI:** 10.1021/jp808774m
18. A. M. Cruz, D. S. Martinez, E. L. Cuellar, *Solid State Sci.*, **12**,88(2010), **DOI:**10.1016/j.solidstatesciences.2009.10.010
19. W. Yu, J. Chen, T. Shang, L. Chen, L. Gu, T. Peng, *Appl. Catal. B,* **219**, 693(2017), **DOI:**10.1016/j.apcatb.2017.08.018.
20. K. Prakash, P. S. Kumar, S. Pandiaraj, K. Saravanakumar, S. Karuthapandian, *J. Exp. Nanosci.,* **11,** 1138(2016), **DOI:**10.1080/17458080.2016.1188222
21. A. B. Murphy, *Sol. Energy Mater. Sol. Cells,* **91**, 1326 (2007), **DOI:**10.1016/j.solmat.2007.05.005
22. M.E. Khan, M.M. Khan, M.H. Cho, *RSC Adv.,* **6**, 20824 (2016), **DOI:**10.1039/C5RA24575C
23. L. Zhang, Y. Li, Q. Zhang, H. Wang, *Cryst. Eng. Comm.,* **15**, 5986(2013), **DOI:**10.1039/C3CE40620B
24. K .Prakash, P. S. Kumar, P. Latha, K. S. Durai, R. Shanmugam, S. Karuthapandian, *Mater. Res. Bull.,* **93**, 112 (2017), **DOI:**10.1016/j.materresbull.2017.04.018
25. P.S. Kumar, M. Selvakumar, S.G. Babu, S. Karuthapandian, *Mater. Res. Bull.*, **83**, 522(2016), **DOI:**10.1016/j.materresbull.2016.06.043
26. K. Prakash, P. S. Kumar, P. Latha, K. Saravanakumar, S. Karuthapandian, *J. Inorg. Organomet. Polym.*, **28**, 268 (2018), **DOI:**10.1007/s10904-017-0715-5
27. P.S. Kumar, M. Selvakumar, S.G. Babu, S. Induja, S. Karuthapandian, *J. Alloy. Compd.*, **701**, 562 (2017), **DOI:**10.1016/j.jallcom.2017.01.126.

, [RJC-3076/2018]